ELSEVIER

Polymer 42 (2001) 8425–8434

polymer

www.elsevier.nl/locate/polymer

Physical and mechanical properties of polyethylene for pipes in relation to molecular architecture. I. Microstructure and crystallisation kinetics

L. Hubert[a], L. David[a], R. Séguéla[a,*], G. Vigier[a], C. Degoulet[b], Y. Germain[c]

[a]*Groupe d'Etudes de Métallurgie Physique et de Physique des Matériaux, INSA, de Lyon Bât. 502, 20 avenue Albert Einstein, 69621 Villeurbanne, France*
[b]*ATOFINA, Groupement de Recherches de Lacq, 64170 Lacq, France*
[c]*ATOFINA, FINA Research, Zone Industrielle C, 7181 Feluy, Belgium*

Received 5 March 2001; received in revised form 30 April 2001; accepted 11 May 2001

Abstract

Ethylene/α-olefin copolymers having bimodal molar weight distribution are investigated in comparison with unimodal copolymers in order to understand the incidence of the molecular architecture on the stress cracking resistance. The preferred introduction of the co-units in the longest chains of bimodal copolymers is suggested to favour the occurrence of intercrystalline tie molecules during crystallisation. The more complex is the molecular architecture, the greater is the difficulty for crystallisation by regular chain folding. Intermolecular chemical heterogeneity resulting from preferred incorporation of the co-units in the long chains enhances the co-unit disturbing effect on crystallisation without reducing crystallinity. Intra-molecular heterogeneity of the co-unit distribution is also suggested to be an efficient means to generate tie molecules and random chain folding at the expense of regular chain folding. Isothermal crystallisation is used to probe the effect of molecular architecture on the crystallisation kinetics. It appeared that the correlations between kinetics, molecular architecture and molecular topology of unimodal copolymers no longer hold when considering bimodal copolymers. In contrast, the crystal surface free energy proved to be sensitive to topological changes resulting from molecular architecture modifications.

Keywords: Polyethylene; Pipe; Bimodal ethylene copolymer

1. Introduction

Since its introduction in pipe applications more than 20 years ago, polyethylene (PE) has been taking a growing place in gas and water distribution due to its low cost, lightness and good corrosion resistance. Besides, long-term properties have been steadily rising due to the development of novel PE-based materials. The present highest standard is the PE100 class, which means that pipes made from such materials should withstand a hoop stress of 10 MPa, for 50 years at room temperature, including a 1.25 safety factor.

Evaluation of long-term properties for certification of such kind of materials cannot reasonably be carried out at room temperature (RT). Conventional stress cracking tests are performed on pressurised pieces of actual pipes at temperatures ranging from 60 to 100°C [1,2]. Such accelerated experiments may yet be extended over about 2 years. The long-term behaviour at RT is extrapolated from the data at higher temperatures, using standard methods. Stress cracking investigations are however often carried out, in creep or fatigue loading, using notched tensile or bending samples which roughly reproduce the plane strain conditions relevant to actual service and which are more convenient than pipe testing [1–21]. Accelerated stress cracking tests are also commonly performed in surfactant environment in order to reduce test time, but transposition of the results for predicting life time of pipes in natural conditions is not straightforward.

Whatever the environment and temperature conditions, high stresses lead to ductile failure of the pipes. After the appearance of a parrot-beak-like deformation zone elongated parallel to the tube axis [6,21], microcracks quickly develop in the region of the highly oriented material, normal to the tube axis. At low stresses, a so-called brittle failure occurs by slow crack growth (SCG) through the tube wall, with the crack plane parallel to the tube axis [6,21]. Ben Hadj Hamouda et al. [21] have clearly shown that such cracks initiate from the inner surface of the tube wall, generally about surface defects or solid particles of residual catalyst or mineral filler.

* Corresponding author.

0032-3861/01/$ - see front matter
PII: S0032-3861(01)00351-2

In the ductile domain, time to failure increases tremendously with decreasing stress, whereas in the brittle domain, time to failure is much less dependent on stress. So, the most important feature of the stress versus failure time plots is the location of the ductile–brittle transition which determines the material life time in service at RT. The mirror-like aspect of the fracture initiation zone of the cracks characteristic of the brittle regime is an indication that the first step of the cracking phenomenon is actually a brittle process [21]. However, the hairy-like surface of the fracture that systematically appears away from the initiation zone of the crack [21] reveals a gradual contribution of plastic processes in the crack propagation, accompanied with a fibrillar transformation of the material at the tip of the propagating crack [7,8,11,12,19–21]. This can be ascribed to the fact that, at constant pressure in the tubes, or constant loading in tensile tests, the local tensile stress steadily increases in the remaining ligament ahead of the propagating crack. Thereby, the local stress state about the crack tip gradually shifts from brittle to ductile behaviour.

Brittle failure has been claimed by a number of authors to originate from chain disentanglement in the fibrils [11–20], seemingly by analogy with the mechanism of craze rupture in glassy polymers close to the glass transition temperature. Chain rupture may however be a likely mechanism for brittle failure. This phenomenon has been assumed to intervene at the initiation step of stress cracking, when the applied stress is much lower than the yield stress [3,7,8]. But borrowing from the models of microfibril rupture in highly drawn semi-crystalline polymers, including PE [22,23], one may also suspect the occurrence of chain breakage during the propagation step involving fibrillation of the material about the crack tip. This standpoint is supported by recent studies from Plummer and Kausch giving evidence that breaking of craze fibrils in semi-crystalline polymers is mainly due to the rupture of stressed chains rather than to the disentanglement of such chains [24,25].

It has often been assumed that intercrystalline tie molecules and entangled chain loops bear most of the load in the rubbery amorphous layers between crystallites in PE, so their concentration should be a prime factor for controlling slow crack growth. As a matter of fact, both high molar weight chains and short chain branches (SCB) that are claimed to increase tie chain frequency after crystallisation do improve long-term behaviour. However, increasing molar weight reduces processability due to viscosity upswing while copolymerisation reduces yield stress due to crystallinity drop, so that improvement of long-term properties from these two parameters turned out limited. The nature of the α-olefin comonomer is another factor of undeniable influence [16], but its precise part on long-term behaviour is not well understood. A promising route to progress in this challenge has been opened in recent years, owing to the opportunity to incorporate the co-units in the high molar weight chains that is inverse to the natural trend of usual catalytic processes. Preferred incorporation of the co-units in long chains was indeed suspected to provide a synergetic effect on lifetime [9,10,17,18,26–28]. Taking advantage from a combination of Ziegler–Natta catalysts with cascade reactors, a new class of PE has been developed, the so-called bimodal or 3rd generation PE. Thereby, the co-unit distribution as a function of chain length turned out to be an additional parameter of the molecular architecture available for tailoring long-term properties, besides co-unit concentration and nature, and molar weight distribution (MWD).

In the present study, we investigate a series of high density PEs for pipe applications having various molecular architectures with the aim to increase the knowledge of the structure–property relationships, and finally contribute to the improvement of end use properties. Crystallisation kinetics is more specifically studied in relation to molecular architecture. Crystallisation is indeed a determining step in the build up of the molecular topology of the solid materials, notably regarding the frequency of intercrystalline tie molecules and chain entanglements. The goal of this work is to establish if crystallisation kinetics may be a reliable means to foresee PE durability in relation to molecular architecture, as previously suggested by some authors [26,29,30]. In this approach, high temperature crystallising species are ascribed a detrimental effect on tie chain formation due to high propensity for regular chain folding.

2. Experimental

Five ethylene/α-olefin copolymers from various sources have been investigated. CP1 and CP2 are produced from a chromium-oxide (CrO_2) catalysis in gas phase. CP4 was synthesised from a slurry Ziegler–Natta (ZN) catalysis. CP3 and CP5 are bimodal ZN copolymers produced in tandem reactors. The materials were compression-moulded into 1 mm thick sheets by melting pellets at 160°C for 5 min, and cooling at about 20°/min. Average molar weights were determined by size exclusion chromatography (SEC) in trichlorobenzene at 150°C. Density data are average values from three measurements carried out in a water–ethanol gradient column. The durability grade of the materials has been determined according to the ISO/TR9080 standard method. The molecular and physical characteristics of the materials are reported in Table 1.

Differential scanning calorimetry (DSC) investigations were performed on a DSC-7 apparatus from Perkin–Elmer at a heating rate of 10°C/min, apart from the isothermal study described below. Calibrations of the temperature and heat flow scales were achieved from the analysis of the melting of high purity indium and zinc samples, at the same heating rate. The melting point, T_f, of the materials was taken at the melting endotherm peak. Crystal weight fractions were determined from heating scans after standard cooling at 10°C/min using the relation $X_c = \Delta H_f/\Delta H_f^0$, where ΔH_f is the specific enthalpy of melting of the material

Table 1
Molecular and physical characteristics of the copolymers

Copolymer	Co-unit/MWD[a]	Methyl (CH_3‰C)	M_n (kg/mol)	M_w (kg/mol)	M_z (kg/mol)	Density (g/cm^3)	Durability grade
CP1	Hexene/UM	4.3	9.3	183	1470	0.940	PE80
CP2	Hexene/UM	1.6	11.7	207	1530	0.946	PE80[b]
CP3	Hexene/BM	2.4	11.8	220	1540	0.948	PE100
CP4	Butene/UM	2.4	9.1	236	1580	0.945	PE63
CP5	Butene/BM	3.5	10.2	215	1160	0.944	PE80

[a] MWD = molar weight distribution; UM = unimodal; BM = bimodal.
[b] CP2 is intermediate between PE80 and PE100 grades of SCG resistance but does not reach the PE100 standard.

Table 2
Thermodynamic and structural characteristics of the copolymers

Copolymer	X_c (wt%)	L_c (nm)	T_f (°C)	σ_e (mJ/m^2)
CP1	58 ± 1	10.2 ± 0.3	128.0 ± 0.3	46 ± 3
CP2	63	12.4	130.0	48
CP3	65	13.2	128.5	58
CP4	67	15.6	131.5	52
CP5	66	16.0	130.5	59

and $\Delta H_f^0 = 290$ J/g that of the perfect orthorhombic PE crystal at its thermodynamic melting point $T_f^0 = 141$°C [31]. The melting enthalpy was determined by linear interpolation of the baseline between the clear-cut end of the melting endotherm and its onset arbitrarily taken at 70°C for all the materials.

Surface free energy of the crystal lamellae, σ_e, was computed from the following Gibbs–Thomson equation

$$T_f = T_f^0(1 - 2\sigma_e/\Delta H_f^0 \rho L_c)$$

in order to get an insight into the topological changes of the chain folding surface of the crystalline lamellae [32]. The most probable crystal thickness, L_c, was assessed from small-angle X-ray scattering (SAXS) using the relation $L_c = LX_c\rho/\rho^*$, which assumes a very large extension of the crystal lamellae as compared to their thickness, with ρ being the density of the material and $\rho^0 = 1.000$ g/cm^3 that of the perfect orthorhombic PE crystal. The SAXS bench was composed of a Rigaku Cu-rotating anode having a 0.1 mm focus and operated at 30 kV and 40 mA, an assembly of two Ni-coated curved mirrors at right angle providing punctual collimation of the incident beam, a position sensitive and Cu Kα energy-selecting linear counter located at 80 cm of the sample, and a vacuum section between detector and sample. The samples consisted of two piled pieces of 1 mm thick sheet for optimum X-ray absorption. The long period, L, was directly computed from the correlation peak of the Lorentz-corrected scattering curve. The thermodynamic and structural data of the five materials are reported in Table 2.

An extensive molecular characterisation of CP1, CP2 and CP3 has been carried out through a preparative temperature rising elution fractionation (TREF) followed by infra-red (IR) determination of the methyl group concentration in the polymer fractions, together with SEC and DSC analyses of the fractions. The TREF experiments were made from 1% polymer solutions in xylene at 130°C. The hot solution was first cooled down at 3°/h. Then elution fractionation was carried out from 10 to 125°C at a heating rate of 20°/h. Seven fractions were collected for every material. The overall methyl group concentration of every fraction was determined from the 1375 cm^{-1} IR band, after subtraction of the spectrum of a high molar weight linear PE having virtually no SCB. Calibration of the band intensity was made from the absorption spectrum of a paraffin having a well-known concentration of methyl end groups. Vinyl end group concentration was determined from the 909 cm^{-1} IR band. The SCB concentration due to the co-units was computed by subtracting to the overall methyl group concentration that of the methyl end group concentration assessed from the number-average molar weight of the fractions, taking into account the vinyl end group concentration. The data are reported in Tables 3–5. SEC and DSC measurements on the fractions were carried out as described above. In the case of DSC melting analyses, the raw powders were first

Table 3
Molecular characteristics of the CP1 fractions from TREF (subscript F holds for fraction)

Fraction	T-range (°C)	X_F (wt%)	Methyl (CH_3‰C)	Vinyl (C_2H_3‰C)	SCB_F (CH_3‰C)	M_n (kg/mol)	M_w (kg/mol)	$SCB_F \times X_F$
F1	10–40	1.1	29.5	10.8	~nil	0.65	10.80	~nil
F2	40–60	0.9	21.2	5.2	3.2	1.20	12.80	0.03
F3	60–80	6.3	17	2.5	10.7	3.20	33.40	0.67
F4	80–93	22.8	8.8	1.8	5.7	5.70	58.00	1.3
F5	93–98	14.7	3.7	0.8	2.5	13.65	97.00	0.36
F6	98–110	9.3	2.1	0.6	1.2	19.20	121.00	0.11
F7	110–125	44.9	~nil	0.3	~nil	45.50	290.00	~nil

Table 4
Molecular characteristics of the CP2 fractions from TREF

Fraction	*T*-range (°C)	X_F (wt%)	Methyl (CH_3‰C)	Vinyl (C_2H_3‰C)	SCB_F (CH_3‰C)	M_n (kg/mol)	M_w (kg/mol)	$SCB_F \times X_F$
F1	10–40	0.7	29	–	~nil	0.55	9.56	~nil
F2[a]	40–60	0.2	–	–	–	1.00	13.98	–
F3	60–80	3.7	10	5.8	2.2	2.28	25.32	0.08
F4	80–93	11.1	6	2.8	2.7	4.76	44.32	0.30
F5	93–98	22.2	1.6	1.0	1.0	14.43	85.67	0.22
F6	98–110	5.0	~nil	0.53	~nil	24.44	131.80	~nil
F7	110–125	57.1	~nil	0.3	~nil	42.00	284.00	~nil

[a] IR measurements not possible on fractions with mass less than 10 mg.

heated up to 170°C for 5 min and then cooled down to RT at 10°C/min.

The isothermal crystallisation study has been carried out on the Perkin–Elmer DSC-7 apparatus according to the following procedure. The samples were heated above the melting point at 170°C for 5 min in order to standardise the physical state of the materials prior to the experiment. Cooling down to the temperature of isothermal treatment was then operated at 30°C/min. This cooling rate was a compromise between fast cooling and minimum delay to reach thermal equilibrium. The temperature domain of investigation 117–122°C allowed crystallisation times ranging from a few tens of seconds at onset to several hours at completion. Time–temperature–transformation (TTT) diagrams were established by plotting crystallisation temperature versus crystallisation time at constant transformation ratios.

3. Results and discussion

3.1. Physical properties versus co-units nature and distribution

Fig. 1 shows the SEC elution curves of CP1 and CP3. The bimodal character of the molar weight distribution of CP3 due to the tandem reactor synthesis is clearly seen, as compared with the unimodal distribution of CP1.

The data from Table 1 show the influence of both the nature and the distribution of the co-units. Comparison of the unimodal CP2 and CP4, on the one hand, and the bimodal CP3 and CP5, on the other hand, reveals that a higher content of butene co-units is required as compared with hexene, to provide similar crystal level, as judged from the methyl group concentration. This is due to the fact that, although partial, the much easier incorporation of butene units in the crystalline phase [33,34] involves lesser disturbance of the regular chain-folding mechanism and of the chain reeling process during crystallisation. These two phenomena have previously been ascribed a major influence on the intercrystalline tie chain and entanglement densities [9,35,36]. In parallel, durability of hexene copolymers CP2 and CP3 turns out to be better than that of CP4 and CP5 butene copolymers, respectively, as already reported [16].

Comparison of data from Tables 1 and 2 shows good agreement between the density data (Table 1) and the crystal weight fractions X_c from DSC measurements (Table 2). However, some disagreement seems to appear when comparing density and X_c data for butene and hexene copolymers: namely CP4 and CP5 have higher X_c values than CP2 and CP3 whereas the former copolymers have lower densities than the latter ones. This is likely due to the fact that butene co-units are able to enter the PE crystal lattice at a rate close to 10 mol% [35], a phenomenon that seemingly affects much more crystal density than melting enthalpy.

We suggest that the major role of the co-unit concentration and nature in long-term behaviour lies on the chain topology modification during crystallisation: the higher the co-unit concentration and bulkiness, the greater chain folding and chain reeling are disturbed. In relation to chain

Table 5
Molecular characteristics of the CP3 fractions from TREF

Fraction	*T*-range (°C)	X_F (wt%)	Methyl (CH_3‰C)	Vinyl (C_2H_3‰C)	SCB_F (CH_3‰C)	M_n (kg/mol)	M_w (kg/mol)	$SCB_F \times X_F$
F1[a]	10–40	0.2	–	–	–	0.48	2.90	–
F2[a]	40–60	0.1	–	–	–	0.80	6.00	–
F3	60–80	0.5	23.9	0.5	6.9	1.60	38.00	0.03
F4	80–90	11.4	11.5	0.3	4.3	3.70	88.00	0.49
F5	90–98	22.2	3.8	0.2	1.2	10.00	140.00	0.27
F6	98–104	13.5	0.8	~nil	~nil	18.00	191.00	~nil
F7	104–125	52.1	~nil	~nil	~nil	34.00	295.00	~nil

[a] IR measurements not possible on fractions with mass less than 10 mg.

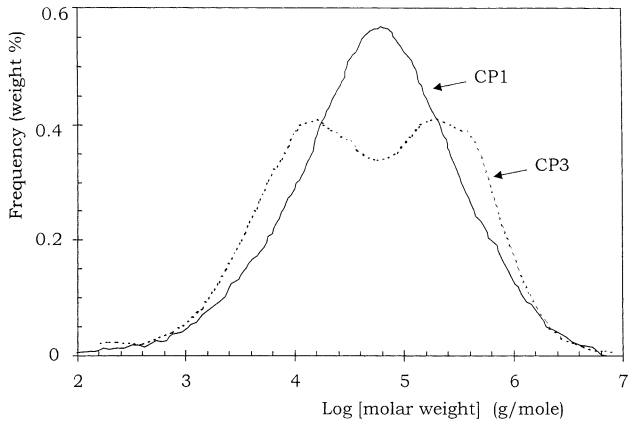

Fig. 1. SEC curves of CP1 and CP3.

architecture, crystallisation determines the tie chain and chain entanglement density of the solid material, and thereby most of its mechanical properties. As a matter of fact, the greater is the concentration of intercrystalline tie chains and entangled chain loops in the amorphous phase, the lower are the local stresses borne by these mechanically active molecular species. This is radically different from the interpretation proposed by many authors following Brown's view that SCG [11–13,27] is mainly governed by chain disentanglement at the tip of the propagating crack, without considering topological changes in the isotropic materials due to the influence of co-unit nature and concentration on crystallisation kinetics. In Brown′s approach, the main effect of co-units on SCG is a reduced rate of chain disentanglement due to the hindrance for dragging the protruding SCB through the crystals [7,12,16,20,28]. Notwithstanding, both phenomena may actually contribute to improve SCG resistance.

Comparison of bimodal and unimodal copolymers having the same kind of co-units, i.e. CP3 versus CP2 and CP5 versus CP4 (see Table 1), shows that a higher co-unit content is required for bimodal copolymers to provide similar crystal level, as previously reported [18]. In parallel, durability is better for the bimodal materials (Table 1). The incorporation of the co-units in the high molar weight chains has been claimed to increase the tie chain concentration, but this has not been given clear evidence. In a recent Raman spectroscopy study on drawn samples of various PE for pipes, Laragon et al. [37] have shown that mechanically active chain portions in all-*trans* conformation are less strained in a bimodal copolymer as compared with equivalent unimodal copolymers. This can be taken as a piece of evidence that tie molecules and chain entanglements are more numerous in a bimodal material, and provides explanation for the improvement of stress cracking resistance [37].

As can be seen from Table 2, bimodal copolymers CP3 and CP5 have slightly higher surface free energy than their unimodal parents of same co-unit type, CP2 and CP4, respectively. This thermodynamic parameter is sensitive to modifications of the chain topology [32,38–40], which in the case of PE crystallites spans from regular chain-folded single crystals to fringed micelles. Due to the assumptions made in the calculations, the σ_e data of Table 2 cannot be taken as absolute values. However, the fact that their departures lie on the second digit of the figures, i.e. above the error due T_f and L_c standard deviations, makes them quite relevant to some changes of the chain topology at the crystal surface. The slightly greater σ_e of bimodal copolymers gives indication that their chain-folding topology is somewhat more irregular than that of the corresponding unimodal copolymers, suggesting more tie molecules and chain entanglements [32]. This modification of the chain topology at the crystal surface is likely to be at the origin of the benefiting effect on long-term behaviour of the co-unit incorporation in the longer chains owing to a modification of the crystallisation mechanisms that will be discussed in Section 3.3.

In the theoretical approach of tie chains proposed by Brown [11,41], the tie chain density is assessed from the probability of chain portions to cross an amorphous layer and the two adjacent crystal lamellae. This approach assumes preservation of the overall random coil topology of the chains from the melt with only local rearrangement of segments to build up the crystalline structure. The determining role of non-crystallisable co-units is ascribed to the reduction of crystal thickness that parallels co-unit content increase [13,41,42]. Indeed, computations predict a drastic increase of tie chain probability as crystal thickness decreases with decreasing crystallinity. So, considering the slightly greater crystal thickness that is observed in Table 2 for bimodal copolymers CP3 and CP5 as compared with the corresponding unimodal copolymers CP2 and CP4, respectively, Brown′s model turns out unable to predict any increase of tie chain concentration that is largely proclaimed for bimodal copolymers as a result of the 'reversed' co-unit distribution. In contrast, our interpretation based on changes in the chain folding mechanism during crystallisation may account for the improved SCG resistance of bimodal copolymers. As will be discussed below in more details, the specific molecular architecture of bimodal copolymers is suspected to induce significant modifications in the chain topology after crystallisation, as compared with unimodal copolymers at equivalent crystallinity and crystal size. Co-units incorporated in longer chains are ascribed to have a synergetic effect to disturb regular chain folding, and thus promote intercrystalline tie chains. No explanation has yet been found for the slightly greater crystal thickness of the bimodal copolymers.

Surface free energy is the unique quantitative support to this interpretation. The σ_e data of Table 2 unfortunately do not exhibit an evolution parallel to the ranking in durability grade of the five copolymers (Table 1). This may be due to the fact that changing the co-unit type involves topological modifications of the crystal surface that should affect

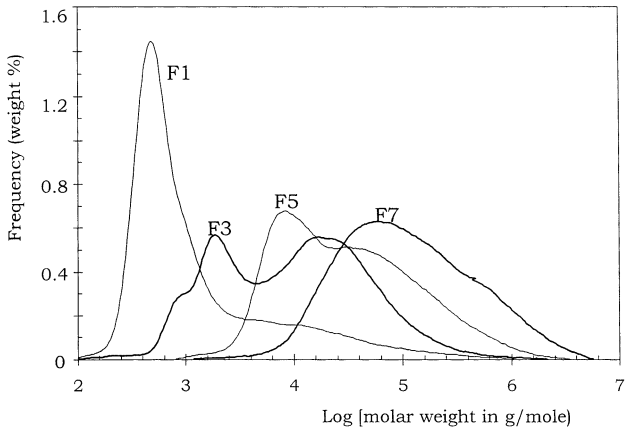

Fig. 2. SEC curves of CP1 fractions from TREF.

surface free energy without necessarily increasing tie chain density. For instance, the co-unit concentration close to the crystal surface should be higher in the case of butene copolymers, which have a higher overall co-unit content than hexene copolymers, at equivalent crystallinity. This is likely to contribute an increase to the surface free energy without improving mechanical properties.

3.2. Analysis of the TREF data

In the search for understanding long-term properties of PE in relation to molecular architecture, the co-unit distribution as a function of chain length cannot be just discussed on a qualitative level of long chains versus short chains. Fractionation by means of TREF proved to be an essential tool to get deeper insight into the molecular architecture of ethylene copolymers [26,27,30,43–49].

From the data of Tables 3–5 referring to copolymers CP1, CP2 and CP3, the global methyl group concentration of every fraction follows a correlation with the median value of the corresponding elution temperature domain that is in quite good agreement with previously reported data on various ethylene/α-olefin copolymers [43,44,50]. It notably decreases with increasing elution temperature, while chain length increases in parallel as judged from the M_n and M_w data of every fraction. It is however noteworthy that, taking into account methyl groups due to main chain ends, the first two fractions F1 and F2 for the three copolymers appear thoroughly or nearly deprived of SCB associated with co-units. This means that methyl groups from both SCB and chain ends play similar depressive effect on the crystallisation temperature. However, when studying SCG, care must be taken to separate the two kinds of methyl groups since SCB associated with co-units are suspected to contribute generating tie chains, while chain ends do not.

A drastic increase of both number-average and weight-average molar weight of the fractions parallels the increase of elution temperature (Tables 3–5). There is however a striking difference between the fractions regarding the distribution of the co-units as a function of the chain molar weight, as can be judged from the $SCB_F \times X_F$ data of Tables 3–5. For CP1 and CP2, about 85–90% of the co-units lie in fractions covering the molar weight ranges $33\,000 < M_w < 97\,000$ (F3–F5) and $44\,000 < M_w < 85\,000$ (F4–F5), respectively. In contrast, 90% of the co-units in CP3 are concentrated in fractions F4–F5 for which chains span the molar weight range $88\,000 < M_w < 140\,000$. For CP3, the co-units are definitively located on longer chains than those of the two other copolymers. The longest chains of the three copolymers are surprisingly homopolymers, as judged from the SCB_F data of the F7 fractions (Tables 3–5) which prove to be nil, within the accuracy of IR experiments.

Using various unimodal ZN type ethylene/hexene copolymers, Soares et al. [30] have recently pointed out that a correlation exists between the SCG resistance and the amount of matter in the fraction that is collected in the 75–85°C elution temperature range. Best performances notably occur for copolymers having more than 50% by weight in a 75–85° fraction. This was ascribed to an optimum efficiency of SCB distribution and chain length on the formation of intercrystalline tie molecules. This correlation does not apply to our unimodal copolymers CP1 and CP2, as well as to the CP3 bimodal copolymer. As a matter of fact, the X_F values of Tables 3–5 show that less than 30% of matter are gathered in the 60–90° elution temperature range for CP1 (i.e. F3 + F4), and even just 14 and 12% for CP2 and CP3, respectively. In fact, more than 60% of the material is collected above 100°C for CP3 (i.e. F6 + F7). The reason for this serious disagreement with the correlation pointed out by Soares et al. may be that both the SCB and the molar weight distributions of the present copolymers are far different from that of the conventional ZN copolymers due to different synthesis processes. The SEC elution curves of the fractions from the preparative TREF reported in Fig. 2 indeed show a strongly marked bimodal MWD for several fraction of the CrO_2-catalysis CP1, in spite of the fact that this copolymer exhibits an overall unimodal character (see Fig. 1). This contrasts with the data reported by Soares et al. [30] for conventional unimodal ZN copolymers. The bimodal, or even trimodal, character of the MWD of some of the fractions from the overall bimodal CP3 is even more striking, as can be seen on the SEC curves of Fig. 3, except for the first two low-temperature fractions F1 and F2 that display much lower polydispersity than the other fractions of CP3 (see Table 5 and Fig. 3). This is also true for CP1 (see Table 3 and Fig. 2).

The DSC analysis of the fractions is likely to bring about informations on the molecular architecture complexity. Figs. 4 and 5 show the DSC heating curves of some solvent-free fractions from the CP1 and CP3 preparative TREF. Fractions F5 and F7 for both copolymers display a single and sharp melting endotherm with peak temperature close to 130°C that is relevant to a crystal lamella population of rather narrow thickness distribution, composed of

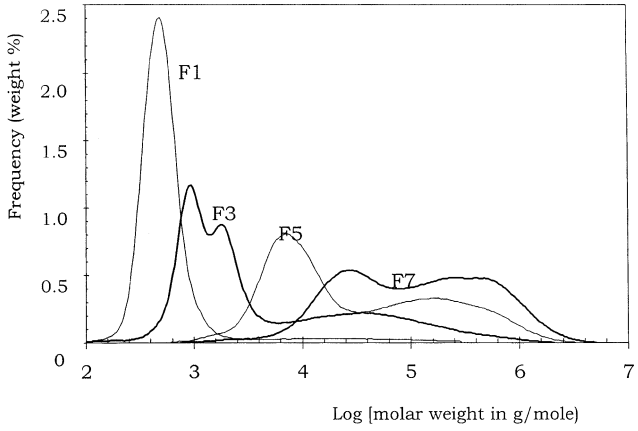

Fig. 3. SEC curves of CP3 fractions from TREF.

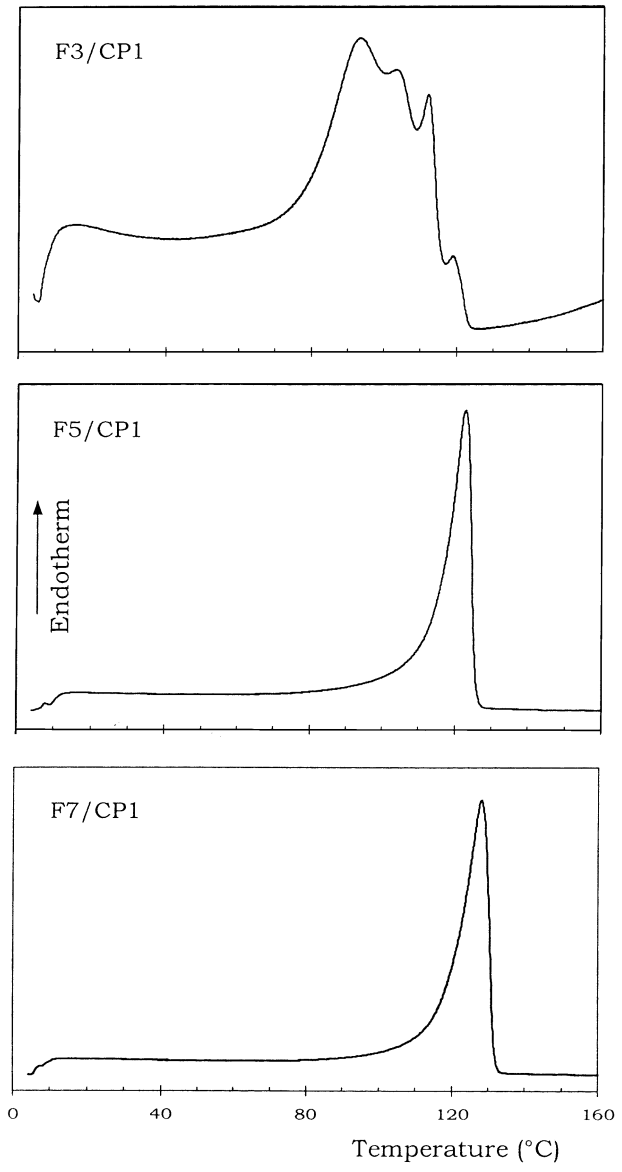

Fig. 4. DSC heating curves of CP1 fractions from TREF (2nd heating scan after melting at 170°C).

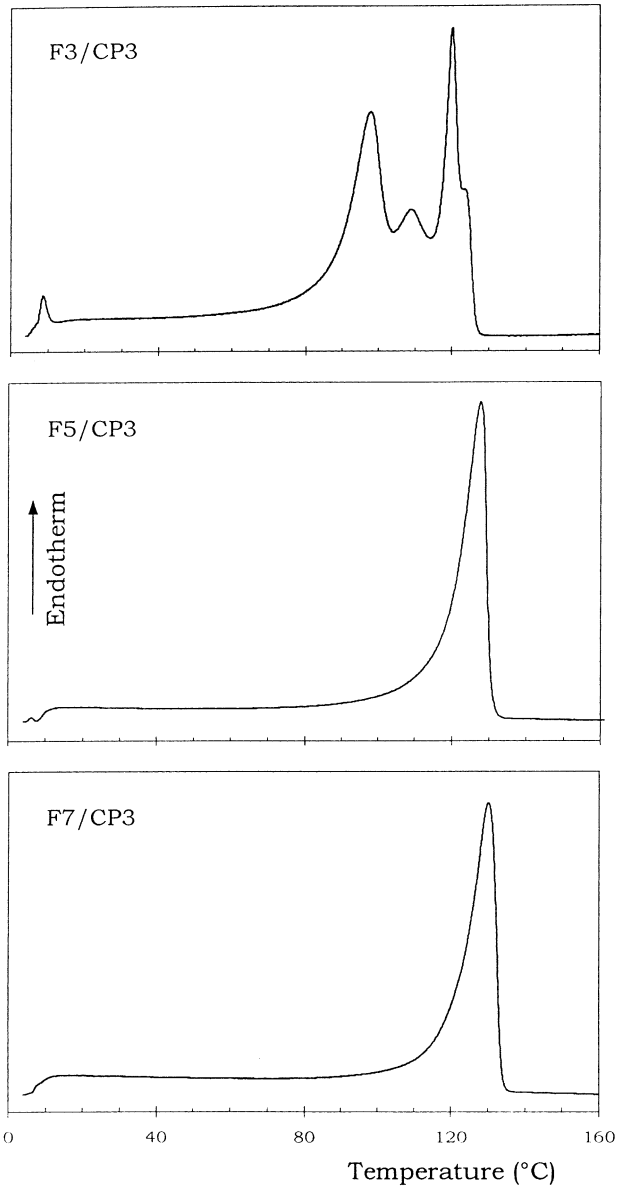

Fig. 5. DSC heating curves of CP3 fractions from TREF (2nd heating scan after melting at 170°C).

molecular species having very low co-unit content. Fractions F7 of both copolymers have even been shown to be composed of nearly pure homopolymers (Tables 3 and 5 show about nil SCB_F data). The surprisingly clear cut bimodal MWD of the F7 fraction of CP3 (Fig. 3) may be due to the introduction of hydrogen as chain transfer agent during polymerisation which generates two chain length populations of homopolymer species. The situation is somewhat more complex for the F5 fraction of CP1 and CP3, which display bimodal MWD (Figs. 2 and 3), sharp melting peak (Figs. 4 and 5) and measurable SCB concentration (Tables 3 and 5). The two populations of chains of the F5 fractions, as revealed by SEC curves of Figs. 2 and 3, are suspected to have slightly different co-unit concentrations

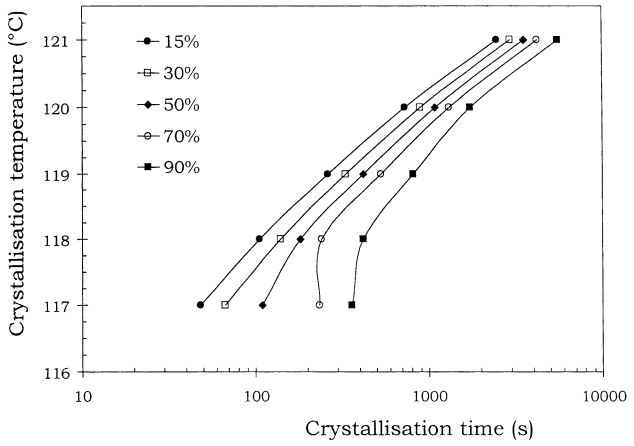

Fig. 6. TTT diagram of CP3 copolymer (every curve refers to constant transformation ratio as indicated).

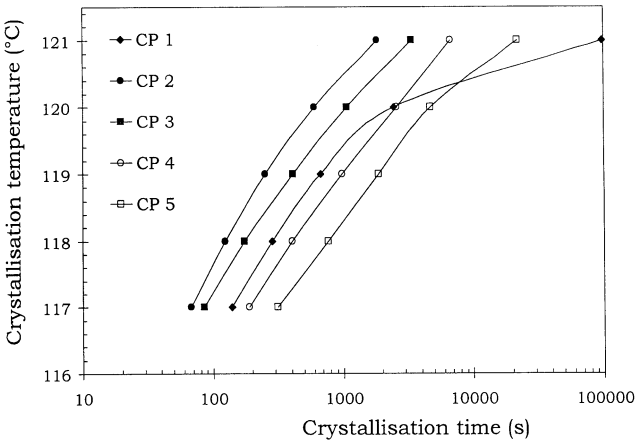

Fig. 7. Partial TTT diagrams of the five copolymers for a 50% transformation ratio.

for compensating the melting point difference due to the molar weight departure of one decade between the two chain populations. Nevertheless, the sharpness of the corresponding melting peak of fractions F5 is strongly suggestive of co-crystallisation of the various species into crystal lamellae of narrow thickness distribution.

Fractions F3 for CP1 and CP3 exhibit a complex and broad melting endotherm, which deserves a specific analysis. Such a melting behaviour is relevant to a blend of chain species having different co-unit contents, and/or significantly different chain lengths. In this instance, considering that paraffins of molar weight about 1 kg/mol have a melting point close to 105°C [31], the lower MW population of the F3 fraction of CP3 (Fig. 3) could be readily ascribed to the lower melting peak of the F3 DSC curve of CP3 (Fig. 5). Regarding the mid and high MW populations of the CP3 fraction F3, at about 2 and 40 kg/mol (Fig. 3), one should expect melting points about 120–125 and 135–140°C, respectively, if they were homopolymers. These figures are notably higher than the observed data of the melting peaks of Fig. 5, indicating that the two chain populations are actual copolymers. This is confirmed by the high SCB_F data of Table 5. A quite important conclusion from these data is that the unlike species that compose the F3 fractions do not co-crystallise into the same lamellae. Phase separation clearly occurs during crystallisation, at least at the scale of the crystalline lamellae. This effect is notably more pronounced for bimodal CP3 than for unimodal CP1.

Regarding molecular architecture complexity, unimodal CrO_2 copolymers turned out surprisingly closer to the bimodal ZN copolymers than to the unimodal ZN ones. In addition, it is to be stressed that the longest chains of fractions F6 and F7 for the three copolymers are deprived of co-units, notably the bimodal CP3. Therefore, if incorporation of the co-units in the long chains proved to be quite efficient for improving long-term properties by increasing the tie molecule concentration, it is clear that there is still room for progress in this way.

3.3. Isothermal crystallisation

An indirect approach to assess the capability of high-density ethylene copolymers to form inter-crystalline tie molecules has been proposed through the study of crystallisation kinetics. The stepwise isothermal segregation (SIS) method consists in the separation in the bulk of the high temperature melting and low temperature melting species corresponding to co-unit poor and co-unit rich chains, respectively. The ratio of the two species was suggested to be an indicator of the long-term behaviour since the co-unit rich part is likely to provide a high rate of tie molecules [26,29]. It turned out that the SIS behaviour of number of high density unimodal copolymers used in early pipe applications displayed good correlation with long-term behaviour.

Isothermal crystallisation was thought to allow comparative evaluation of chain topology. Fig. 6 shows a partial TTT diagram of copolymer CP3. Every curve gives the crystallisation temperature versus crystallisation time relationship at constant transformation ratio, as indicated. At high temperature, slow crystallisation kinetics corresponds to the so-called crystallisation Regime II according to Hoffman [51,52], involving a high rate of regular chain folding accompanied with significant chain disentanglement. In contrast, at low temperature, fast crystallisation kinetics occur in the crystallisation Regime III [52], which prevents chain disentanglement and generates a high frequency of random chain folding and tie molecules. Several pieces of evidence of this topological effect have been indirectly provided from mechanical experiments on linear polymers such as polyethylene [53], polypropylene [54] and polyoxymethylene [55].

Comparison of ethylene copolymers affords valuable informations on their topological behaviour. Fig. 7 shows the TTT diagrams for the five copolymers under investigation. For the sake of clarity and convenience, only plots of the time at the peak of the crystallisation exotherm as a

function of temperature are displayed. The time at peak is indeed very close to the 50% crystallisation time.

Considering the hexene copolymers, CP1 has the lower crystallisation kinetics over the investigated range of temperature, due to higher non-crystallisable SCB content and concomitant lower crystallinity potential. CP2 has the faster rate. Surprisingly, CP3 lies in between, in spite of its slightly higher crystallinity. This observation is consistent with the greater SCB content of CP3 as compared with CP2. As a matter of fact, at equivalent crystallinity, the incorporation of the co-units in the longest chains during polymerisation of bimodal copolymers has already been reported to allow a higher overall co-unit content [18], which in turn is expected to reduce the crystallisation kinetics of these long chains that otherwise have faster kinetics than short chains [56]. The fact that the TTT plot for CP3 (Fig. 7) does not follow the trend of CP1 and CP2 is ascribed to its molecular architecture of so-called bimodal copolymer which no longer allows a correlation between long-term behaviour and crystallisation kinetics when compared with conventional unimodal copolymers. The lower kinetics of CP3 as compared with CP2 (Fig. 7) is notwithstanding clearly indicative of a greater hindrance to regular chain folding at the same temperature.

Regarding the butene copolymers, it appears that the same trend of slower crystallisation kinetics occurs for bimodal CP5 as compared with unimodal CP4 (Fig. 7), in spite of equivalent crystallinity and similar molar weights. This confirms the above conclusion that the preferred incorporation of the co-units in the long chains of bimodal copolymers brings about a perturbing effect on crystallisation accompanied with a hindrance to regular chain folding.

The significant departure of the CP4 and CP5 butene copolymer kinetics from that of the corresponding CP2 and CP3 hexene copolymers (Fig. 7) is undoubtedly due to the higher co-unit content in the former. It seems that, irrespective of occlusion or exclusion from the crystal lattice, butene co-units significantly slow down crystallisation due to the hindrance to the local rearrangement of the chain segments depositing on the growth surface of the crystal. In contrast, butene co-units seem less efficient in disturbing the chain folding mechanism as judged from the surface free energy data.

4. Concluding remarks

It has been accepted for sometime that the preferential introduction of the co-units in the longest chains of ethylene copolymers favours the occurrence of tie molecules during crystallisation. The reason seems that the more complex the molecular architecture, the greater is the difficulty for crystallisation by regular chain folding, and the higher is the hindrance to chain disentanglement during crystallisation. Co-units on long chains are likely to have a combined effect for hindering crystallisation without reducing crystallinity. Bimodal ethylene copolymers actually display better stress cracking resistance than equivalent unimodal copolymers having the same type of co-units and similar crystallinity. Unimodal CrO_2 copolymers look more like bimodal ZN copolymers than unimodal ZN copolymers, regarding molecular architecture complexity. They however have most of the co-units incorporated on shorter chains in comparison with bimodal copolymers.

The high-temperature crystallisation fractions F7–F5 of both unimodal and bimodal copolymers that gather the major part of the materials turned out to contain low co-unit concentrations, if any, and multimodal molar weight distributions. Nevertheless, the different molecular species of these fractions give rise to co-crystallisation that is beneficial for producing intercrystalline tie molecules. In contrast, the F3 fractions clearly exhibit phase separation at the scale of the crystalline lamellae. This is particularly detrimental for tie molecules. This effect that is more pronounced for bimodal copolymers may be the cause of some peculiar mechanical and morphological features of the drawn materials discussed in the following paper of this series [57].

Another level of molecular complexity lies in intra-molecular heterogeneity of the co-unit distribution that should be as efficient as inter-molecular heterogeneity for generating tie molecules and random chain folding at the expense of regular chain folding. Indeed, if co-crystallisation of the co-units in the PE crystal lattice is unlikely, notably for hexene co-units, the chain portions of various co-unit content in a given chain will do their best to crystallise with parent species of unlike entangled chains and give rise to crystallites of various crystal thickness, depending on the lengths of the crystallisable methylene sequences. This intra-molecular segregation of chemical species is likely to increase the frequency of inter-crystalline tie molecules, as compared to the case of inter-molecular heterogeneity only. Such a topological incidence of chemical heterogeneity has been previously inferred by Gedde et al. [58] from solvent extraction experiments on various kinds of PE.

In contrast to this, the rather uniform distribution of the co-units in metallocene copolymers proved to be more efficient in disturbing the regular chain folding mechanism during crystallisation. This was demonstrated through the greater surface free energy of the crystals and the significantly higher strain-hardening behaviour of the metallocene copolymers, as compared with conventional unimodal ZN copolymers [40,59]. Unfortunately the narrow MWD of such materials requires keeping average molar weight to relative low values for acceptable melt processing capabilities. This constraint turned out prejudicial to long-term properties.

In the search to improve long-term properties of ethylene copolymers for pipes, the successful introduction of the co-units in the longest chains has only been achieved by means of tandem reactors leading to the so-called bimodal copolymers. However, it turns out that the longest

chains in such bimodal copolymers issued from conventional ZN or CrO_2 catalysts are thoroughly deprived of co-units, so that there is still openings to progress in the field of new PE synthesis.

Anticipating which process is liable to provide an optimised copolymer architecture for the best long-term behaviour of copolymers is still not an obvious task. Metallocene catalysis, combined with tandem reactors, may be the next route for this challenge [60].

Acknowledgements

The Conseil Régional Rhône-Alpes is deeply acknowledged for the grant of a doctoral fellowship to L. Hubert. The authors are also indebted to L. Murino from ATOFINA (Serquigny) for the detailed infrared analysis of the TREF fractions.

References

[1] Kausch H-H. Polymer fracture. Berlin: Springer, 1987. Chap. 1.
[2] Gedde UW, Viebke J, Leijström H, Ifwarson M. Polym Engng Sci 1994;34:1773–87.
[3] Hannon MJ. J Appl Polym Sci 1974;18:3761–7.
[4] McRae MA, Maddams WF. Makromol Chem 1976;177:473–84.
[5] Crissman JM, Zapas LJ. Polym Engng Sci 1979;19:99–103.
[6] Choi S, Broutman LJ. Proceedings of the 44th ANTEC Conference of the Society of Plastic Engineers, Boston, MA, April 1997. p. 592–9.
[7] Lustiger A, Markham RL. Polymer 1983;24:1647–54.
[8] Lustiger A, Corneliusen RD. J Mater Sci 1987;22:2470–6.
[9] Lustiger A, Ishikawa N. J Polym Sci, Polym Phys 1991;29:1047–55.
[10] Ishikawa N, Shimizu T, Shimamura Y, Goto Y, Omori K, Misaka N. Proceedings of the 10th Plastic Fuel Gas Pipe Symposium of the American Gas Association, New Orleans, LA, 1987. p. 175–83.
[11] Huang YL, Brown N. J Mater Sci 1988;23:3648–55.
[12] Lu X, Wang X, Brown N. J Mater Sci 1988;23:643–8.
[13] Huang YL, Brown N. J Polym Sci, Polym Phys 1990;28:2007–21.
[14] Lu X, Brown N. J Mater Sci 1990;25:29–34.
[15] Zhou Z, Brown N. Polym Engng Sci 1993;33:1421–5.
[16] Yeh JT, Chen J-H, Hong H-S. J Appl Polym Sci 1994;54:2171–86.
[17] Saeda S, Suzaka Y. Polym Adv Tech 1995;6:593–601.
[18] Berthold J, Böhm LL, Enderle H-F, Göbel P, Lüker H, Lecht R, Schulte U. Plast Rubber Compos Process Appl 1996;25:368–72.
[19] Shah A, Stepanov EV, Klein M, Hiltner A, Baer E. J Mater Sci 1998;33:3313–9.
[20] Shah A, Stepanov EV, Capaccio G, Hiltner A, Baer E. J Polym Sci, Polym Phys 1998;36:2355–69.
[21] Ben Hadj Hamouda H, Simoes-Betbeder M, Grillon F, Blouet P, Billon N, Piques R. Polymer 2001;42:5425–37.
[22] Peterlin A, Intern J. Fracture 1975;11:761–80.
[23] Zhurkov SN, Kuksenko VS. Int J Fract 1975;11:629–39.
[24] Plummer CJG, Kausch H-H. J Macromol Sci, Phys B 1996;35:637–57.
[25] Plummer CJG, Kausch H-H. Macromol Chem Phys 1996;197:2047–63.
[26] Scholten FL, Rijpkema HJM. Proceedings of the Plastics Pipes VIII Conference of the Plastics and Rubber Institute, vol. C2/4, Koningshof, The Netherlands, September 1992. p. 1–10.
[27] Brown N, Lu X, Huang Y, Harrison IP, Ishikawa N. Plast Rubber Compos Process Appl 1992;17:255–8.
[28] Clutton EQ, Rose LJ, Capaccio G. Plast Rubber Compos Process Appl 1998;27:478–82.
[29] Gueugnaut D, Rousselot D. Proceedings of the Plastic Piping Systems for Gas Distribution International Symposium of the Gas Research Institute, Lake Buena Vista, FL, October 1997. p. 185–91.
[30] Soares JBP, Abbott RF, Kim JD. J Polym Sci, Polym Phys 2000;38:1267–75.
[31] Wunderlich B. Crystal melting, Macromolecular physics, vol. 3. New York: Academic Press, 1980. Chap. 8.
[32] Darras O, Séguéla R. Polymer 1993;34:2946–50.
[33] Hosoda S, Nomura H, Gotoh Y, Kihara H. Polymer 1990;31:1999–2005.
[34] Gaucher V, Séguéla R. Polymer 1994;35:2049–55.
[35] Séguéla R, Rietsch F. Polymer 1986;27:703–8.
[36] Séguéla R, Rietsch F. J Mater Sci 1988;23:415–21.
[37] Laragon J, Dixon NM, Gerrard DJ, Reed W, Kip B. Macromolecules 1998;31:5845–52.
[38] Wunderlich B. Crystal nucleation, growth, annealing. Macromolecular physics, vol. 2. New York: Academic Press, 1976. p. 30–3.
[39] Flory P, Yoon DY, Dill KA. Macromolecules 1984;17:862–8.
[40] Gaucher-Miri V, Elkoun S, Séguéla R. Polym Engng Sci 1997;37:1672–83.
[41] Huang YL, Brown N. J Polym Sci, Polym Phys 1991;29:129–37.
[42] Zhou Z, Lu X, Brown N. Polymer 1993;34:2520–3.
[43] Usami T, Gotoh Y, Takayama S. Macromolecules 1986;19:2722–6.
[44] Schouterden P, Groeninckx G, Van der Heijden B, Jansen F. Polymer 1987;28:2099–104.
[45] Mathot V, B F, Pijpers MFJ. J Appl Polym Sci 1990;39:979–94.
[46] Wilfong DL, Knight GW. J Polym Sci, Polym Phys 1990;28:861–70.
[47] Hosoda S, Uemura A. Polym J 1992;24:939–49.
[48] Karbashewski E, Kale L, Rudin A, Tchir JW, Cook DG, Pronovost JO. J Appl Polym Sci 1992;44:425–34.
[49] Kim Y-M, Park J-K. J Appl Polym Sci 1996;61:2315–24.
[50] Cady LD. Plast Engng 1987;43:25–7.
[51] Hoffman JD, Guttman CM, Di Marzio EA. Faraday Discuss Chem Soc 1979;68:177–97.
[52] Hoffman JD. Polymer 1983;24:3–26.
[53] Gedde UW, Jansson J-F. Polymer 1985;26:1469–76.
[54] Greco R, Coppola F. Plast Rubber Process Appl 1986;6:35–41.
[55] Plummer CJG, Menu P, Cudré-Mauroux N, Kausch H-H. J Appl Polym Sci 1995;55:489–500.
[56] Shroff R, Prasad A, Lee C. J Polym Sci, Polym Phys 1996;34:2317–33.
[57] Hubert L, David L, Séguéla R, Vigier G, Corfias-Zuccalli C, Germain Y. J Appl Polym Sci, submitted for publication.
[58] Gedde UW, Eklund S, Jansson J-F. Polymer 1983;24:1532–40.
[59] Elkoun S, Gaucher-Miri V, Séguéla R. Mater Sci Engng 1997;A234–236:83–6.
[60] Knuuttila H, Lehtinen A, Salminen H. In: Schiers J, Kaminsky W, editors. Metallocene based polyolefins: preparation, properties and technology, vol. 2. New York: Wiley, 1999. p. 365–78.